Proceedings of 20th International Congress on Acoustics, ICA 2010

23–27 August 2010, Sydney, Australia

Reduction of computing time by genetic algorithm for the nondestructive technique to detect a crack in a large scale concrete structure

Tatsuro Fujiwara, Toyota Fujioka, Yoshifumi Nagata and Masato Abe

Department of Electrical Engineering and Computer Science,
Iwate University, 4-3-5 Ueda, Morioka, 020-8551 Japan

PACS: 43.40.Le, 43.60.Rw

ABSTRACT

As described in this paper, we present a method for estimating the position of a crack in a large concrete structure using several accelerometers. An accelerometer array is installed in the concrete structure and a low-frequency vibration is produced with a small impulse hammer. A reflection wave is thereby generated from any crack that exists in the structure. Because the concrete structure is elastic, it has three wave-propagation modes: the surface-wave mode, the primary-wave mode, and the secondary-wave mode. It is difficult to estimate the position precisely because the power of the necessary primary-wave mode is weaker than that of surface-wave mode. To estimate the crack position precisely, we have proposed a method for eliminating the unwanted surface-wave and side-wall reflections, in which five parameters are used to estimate a single unwanted surface-wave or a side-wall reflection using the least mean squares technique. Because of the long time necessary to estimate even a single unwanted wave (a surface-wave or a side-wall reflection) however, the method is not practical if two or more waves mutually overlap: for instance, 10 parameters are necessary if two waves overlap. Therefore, we propose the use of genetic algorithms (GA). Results show that our method reduces the processing time remarkably. We were able to distinguish two waves reflected from the two close boundaries of a caisson.

INTRODUCTION

Structural health monitoring techniques have been developed to detect (1) the presence or absence of cracks, (2) crack positions, and (3) crack sizes in large structures such as tunnels, dams, and buildings. For such applications, an approximate evaluation of the position and crack size is sufficient. Nondestructive methods of finding a crack in a concrete structure are classifiable into modes using (1) X-rays, (2) IR thermography, and (3) vibration signals. The first type of method cannot locate small cracks such as a thin plate. The second requires that the measuring point be viewed directly. Moreover, neither of the two methods is useful for finding cracks deep within a structure. The third type of method has been widely investigated. In conventional methods, low-frequency vibration signals are driven into the concrete structure by an impact force to estimate the resonance frequency of the concrete structure. Thereby, the position of the crack is estimated. However, this method only works well for some cases in which (1) the crack resembles a sheet and the sheet is parallel to the structure surface (a standing wave is generated in this case), or where (2) the crack is large so that it causes a shift in the resonant frequency. We have already proposed several methods for estimating the position of a sheetlike crack in a concrete structure using several accelerometers. Using such methods, the position of the first reflection wave from the crack caused by the impact force is used to find the crack position instead of the resonant frequency. The positions of cracks can be estimated using this method when the concrete structure has more than one crack, although it is very difficult to estimate their locations using the other conventional methods. Because the concrete structure investigated in our project is very large (larger than 1 m), we use a low-frequency vibration signal instead of an ultrasonic one. This method works well even when the sheetlike crack is slanted to the surface of the concrete structure. In our method, an array of accelerometers is attached to the concrete structure. Then an impact into the concrete structure is made by striking the surface with an impulse hammer. The impact of the hammer produces low-frequency components of less than 10 kHz, which only slightly decrease in power during propagation in contrast to higher-frequency components. Therefore, the reflections from a crack are detectable even if the crack is located deep within the structure. Because the concrete structure is elastic, three wave-propagation modes exist: the surface-wave mode, the primary-wave mode, and the secondary-wave mode. The necessary primary-wave mode is weak compared to the unwanted surface-wave mode. This problem is negligible in the conventional method, which estimates the resonant frequency, but it is a significant obstacle in our method. To estimate the crack position precisely, we proposed a method for eliminating the unwanted surface-wave and side-wall reflections. The method uses five parameters to estimate a single unwanted surface-wave or a side-wall reflection using the least mean squares technique. However, because it takes a very long time to estimate even a single unwanted wave (a surface-wave or a side-wall reflection), the method is not practical if two or more waves mutually overlap: for example, 10 parameters are necessary if two waves overlap. Therefore, we propose herein the use of a genetic algorithm (GA). Results show that the processing time was shortened dramatically compared to the processing time for conventional methods. We were able to distinguish two waves reflected from two close boundaries of a caisson.

MEASURING METHOD

Figure 1 shows the measurement system. The measuring flow is the following:

1. A concrete specimen is struck with a small impulse hammer.
2. Elastic waves propagating through the specimen are received by accelerometers installed on the specimen surface.
3. The accelerometer output and the output of the impulse hammer are fed into a computer through an analog–digital converter.

Three-mode waves (primary wave, secondary wave, and surface wave) are generated by striking the surface of a concrete structure with the hammer. The primary wave and the secondary wave propagate through the concrete structure, and the surface wave propagates on the surface of the concrete structure. A primary wave is a longitudinal wave and a secondary wave is a transverse wave. The accelerometers cannot receive the secondary wave reflected from a crack directly underneath the accelerometers because the accelerometers are one-axis sensors of vertical direction and the reflected secondary wave vibrates mostly in a horizontal direction. In contrast, the accelerometers can receive a primary wave reflected from the crack because it vibrates mainly in a vertical direction. Therefore, the primary wave is used to detect the crack. The power of the primary wave and the secondary wave decrease in proportion to the square of the propagation distance, although the power of the surface wave decreases in proportion to the propagation distance. Consequently, the surface wave becomes dominant at positions far from the impact point. The surface wave might be detected because it decays before the reflected primary wave returns from the crack if a crack position is very deep. If a crack position is shallow, however, then the reflected primary wave returns before the surface wave decays sufficiently. In this case, the crack position detection is difficult because of surface wave interference. Therefore, we describe the method for estimating and eliminating the surface waves in the next section.

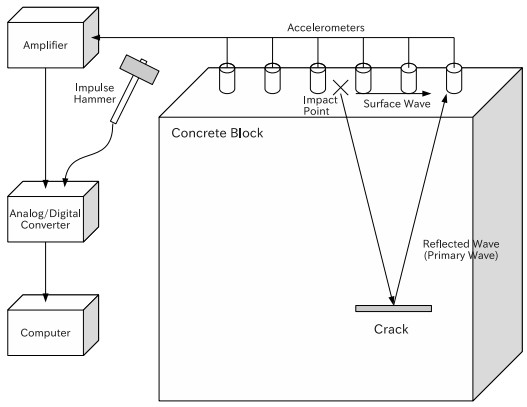

Figure 1: Measurement system.

SURFACE WAVE ELIMINATION

Surface-wave velocity estimation

A surface wave propagates on the surface of a concrete structure at the velocity of about 2000 m/s [8]. However, it changes according to the concrete constituents (amount of water and aggregate contained in the concrete). Accordingly, several accelerometers are actually installed on a concrete structure. Then the velocity of the surface wave is first investigated: First, the propagation distance of the surface wave was calculated from the position of the impact point and the accelerometers. Because the velocity of the surface wave is about 2000 m/s, it is easy to determine which peak in the output of the accelerometer is the peak attributable to the surface wave. This process is conducted for all accelerometer outputs, and the position of the peak caused by the surface wave is located. Then, the time differences between the peaks in the accelerometer outputs are calculated as shown in Fig. 2, from which the surface wave velocity can be evaluated using the least squares method.

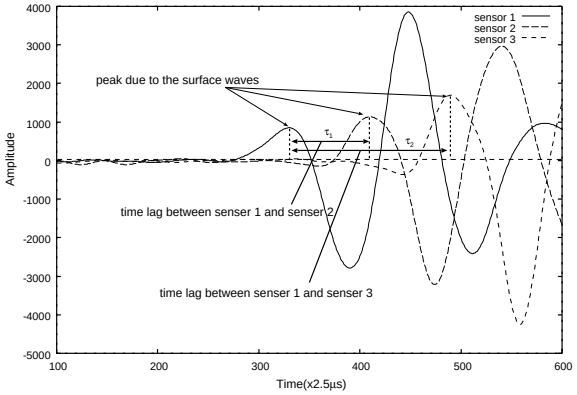

Figure 2: Surface-wave velocity estimation.

Calculation of the surface-wave propagation time

The propagation distance (d_s) from the impact point to each accelerometer is known and the velocity (c_s) of the surface wave was evaluated using the method described in the preceding subsection. Then, the propagation time (τ_s) of the surface wave is expressed as

$$\tau_s = \frac{d_s}{c_s}. \tag{1}$$

Therefore, we can estimate when the direct or reflected surface wave reaches the accelerometer array.

Estimation and elimination of a surface wave

From an experiment on a dam as a huge concrete structure with no crack or reflection, results showed that the impulse response from the output of the impulse hammer to the output of an accelerometer can be regarded as an exponentially decaying sinusoidal wave:

$$h(n) = \alpha \cdot \exp(-\beta n) \cdot \cos(\frac{2\pi n}{T} + \theta), \tag{2}$$

where n stands for the time, α signifies the amplitude of the surface wave, β denotes the decaying coefficient of the surface wave, T represents the period of the surface wave, and θ is the phase of the surface wave. The output $x(n)$ of the impulse hammer was delayed by the propagation time τ evaluated using the method presented in the subsection above. The estimated waveform $y'(n)$ is expressed as follows using the delayed waveform and the impulse response $h(n)$.

$$y'(n) = \sum_{p=0}^{N-1} x(n-\tau-p)h(p) \tag{3}$$

In that equation, N is the length of the impulse response $h(n)$. Here, the original output $y(n)$ of the accelerometer passed through a charge amplifier in the experiment, and the effect of the charge amplifier should be compensated. The charge amplifier serves as a kind of a high-pass filter. Therefore, the difference $x'(n)$

$= x(n) - x(n-1)$ of the impulse hammer output (impact force) was used as the simplest high-pass filter instead of the original output $x(n)$ of the impulse hammer. The estimated surface wave $y''(n)$ using $x'(n)$ instead of $x(n)$ is expressed as

$$y''(n) = x'(n-\tau) * h(n). \tag{4}$$

The five parameters α, β, T, θ, and τ are determined using the least mean squares technique so that the error E becomes minimum.

$$E = \sum_n |y''(n) - y(n)|^2 \tag{5}$$

In Eq. (5), the duration of the summation Σ_n is chosen so that only the surface wave appears in the duration. In the conventional method, each parameter was changed to minimize E, which takes too much time. Therefore, we proposed the use of GA for reducing the computing time.

EXPERIMENT

For confirming the usefulness of GA, we applied GA to the experimental data obtained for a caisson; it is a huge concrete structure used as a breakwater in the sea. The measurement time was reduced to 1/100 (from 48 hours to 30 minutes). This method becomes practical.

Measurement of data

Data measurement was performed in Aomori, Japan. Data were measured for a new caisson set in the ground. It had no cracks. Figure 3 shows both the caisson size and the location of the accelerometer arrays, and Fig. 4 shows the top view indicating the detailed positions of the accelerometer arrays and the impact points. Accelerometers were attached at regular intervals in the middle of the side wall. The top surface of the caisson was struck with an impulse hammer.

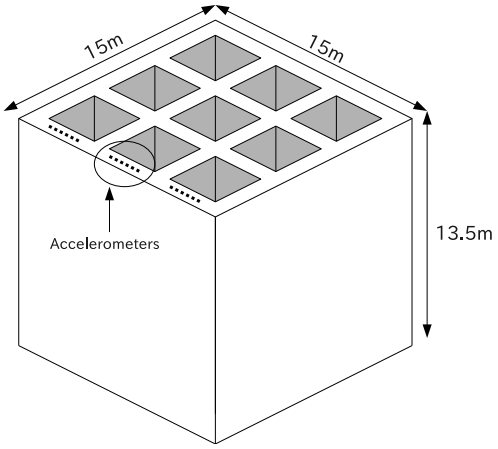

Figure 3: Size of the caisson.

Data analysis

Analyses were conducted using data obtained when the area to the left of the first accelerometer was struck with the impulse hammer, as shown in Fig. 4. The surface wave velocity, as measured using the method described above, was about 2200 m/s. The three surface waves (the direct surface wave and the two surface waves reflected from the nearest side walls depicted in Fig. 5.) were estimated simultaneously. In Fig. 8 the "first estimated waveform" is the sum of the estimated three surface waves, and "first residue waveform" is the signal obtained by subtracting "the first estimated waveform" from the original

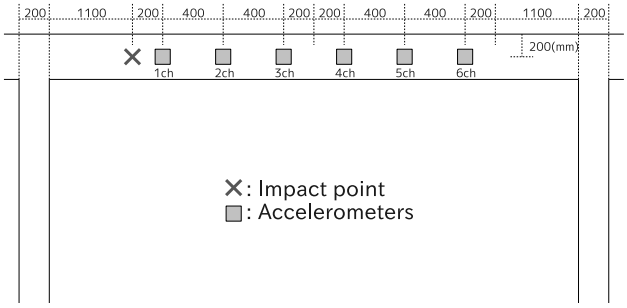

Figure 4: Accelerometer positions and the impact point.

waveform. "Estimated impulse 1" in Fig. 8 is the estimated impulse where the convolution of the impulse and the impulse response $h(n)$ represents the estimate of the accelerometer output attributable to the direct surface wave. The "estimated impulse 2" in Fig. 8 is the estimated impulse, where the convolution of the impulse and the impulse response $h(n)$ represents the estimate of the accelerometer output attributable to the sum of the two reflected waves from the nearest side walls. In Fig. 8, the amplitude of "estimated impulse 1" represents the magnitude of the incident wave because of the direct surface wave. The difference between the position of the "estimated impulse 1" and that of the peak in the impulse hammer output represents the propagation delay.

Second, the two surface waves reflected from the two joints T1 and T2 shown in Fig. 6 were also estimated simultaneously from the residue wave. Figure 9 shows the sum of the reflection waves from T1 and T2 and the second residue, which was generated by subtracting the estimated two waves (reflections from T1 and T2) from the first residue. Figure 10 shows the original waveform and the "2nd residue waveform, from which results show that the error in estimating the surface waves is sufficiently small.

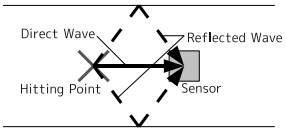

Figure 5: Direct and reflected waves from the nearest side walls.

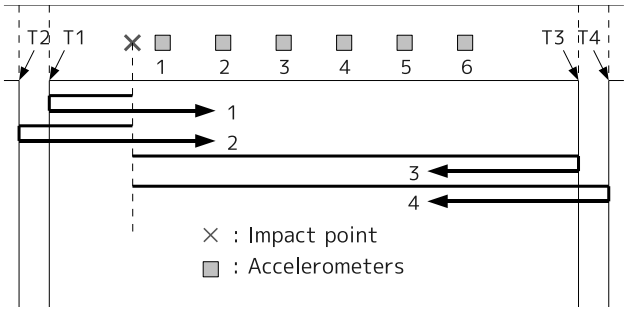

Figure 6: Reflections from joints.

To evaluate the error quantitatively, the power ratio D was calculated for all the accelerometer output except for the #1 and #6 accelerometers.

$$D = 10 \cdot \log_{10} \sum_{n=N_S}^{N_E} \frac{\{B(n)\}^2}{\{A(n)\}^2}, \tag{6}$$

where $A(n)$ stands for the original output, $B(n)$ denotes the residual calculated by our method, and N_S and N_E were set so

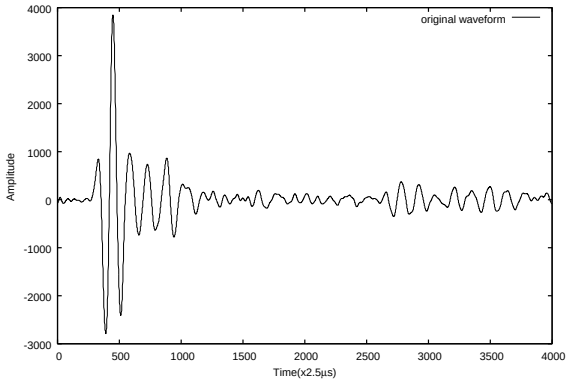

Figure 7: Original waveform of the second (CH #2) accelerometer output.

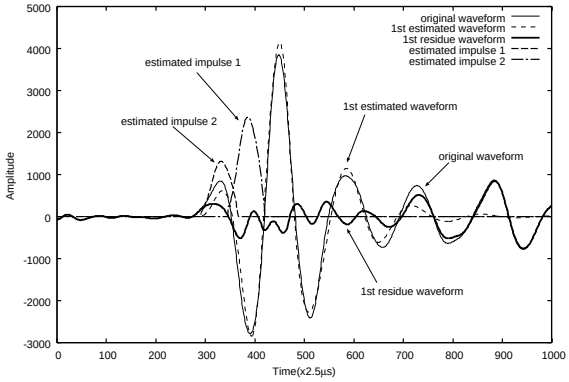

Figure 8: First estimation result (the sum of the direct surface wave and the surface wave reflected from the nearest side wall) obtained using GA.

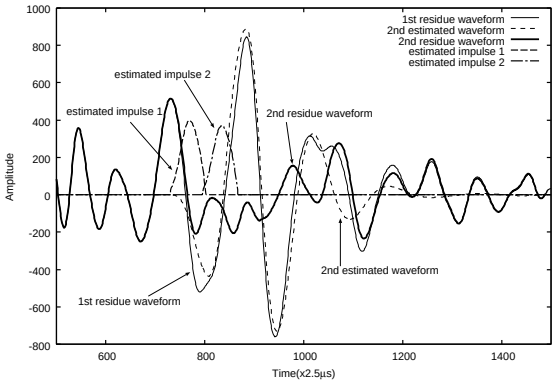

Figure 9: Second estimation result (surface waves reflected from joints T1 and T2) obtained using GA.

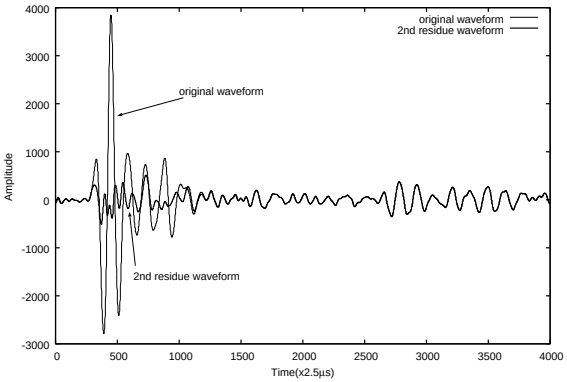

Figure 10: Original waveform of the second (CH #2) accelerometer and its residual waveform.

that only the waves that are considered exist in the calculation. Tables 1 and 2 respectively depict the ratio D for evaluating the error in the first estimation and in the second estimation. In the first estimation, where the direct surface wave and the reflections from the nearest side walls were removed, the ratio D was about -15 dB. Therefore, the direct surface waves and reflections from the nearest side walls were estimated correctly. In the second estimation, where the reflections from T1 and T2 were removed similarly, the ratio D was -7 dB for #2 and #3 accelerometers, it was -14 dB for #4 and #5 accelerometers. The difference arises because the reflection waves from T1 and T2 overlap in the former cases with the rear part of the direct surface wave and reflections from the nearest side walls.

Estimation of refection point

Because the T1 and T2 joint positions are known and the velocity of the surface wave was evaluated using the method described in the former subsection, the propagation delay can be estimated. Tables 3 and 4 show calculated and measured propagation delays for the reflection from T1 and T2, respectively, where the calculated delay means that it was calculated from the positions of the joints and the velocity of the surface wave; the measured one signifies the difference between the position of the "estimated impulse 1" or "estimated impulse 2" in the second estimation results and the position of the peak in the hammer output. Table 3 also presents the error in the propagation delay, which is large for the cases of accelerometers #2 and #3 because the reflection from T1 overlaps with the rear part of the direct surface wave and reflection from the nearest side walls. In Table 4, the error in the propagation delay into large is shown for the cases of accelerometer #4 and #5 because the reflection from T2 overlaps with the reflections from joints T3 and T4.

To reduce the error in the propagation delay for this case, the four reflection waves were estimated simultaneously ($4 \times 5 = 20$ parameters were used). Table 5 presents the calculated and measured propagations and their error for accelerometers #4 and #5. The error was reduced dramatically.

Table 1: Ratio D in the first estimation.

accelerometer	N_S	N_E	D
CH#2	290	730	-16.1
CH#3	380	820	-15.4
CH#4	460	900	-14.0
CH#5	520	960	-15.7

Table 2: Ratio D in the second estimation.

accelerometer	N_S	N_E	D
CH#2	730	1430	-7.0
CH#3	790	1380	-8.3
CH#4	900	1300	-13.1
CH#5	960	1200	-15.7

Table 3: Calculated and measured propagation delays for reflection from joint T1.

accelerometer	T1		
	calculated	measured	error
CH#2	554	563	9
CH#3	625	633	8
CH#4	697	698	1
CH#5	768	769	1

Table 4: Calculated and measured propagation delays for reflection from joint T2.

accelerometer	T2		
	calculated	measured	error
CH#2	625	628	3
CH#3	697	702	5
CH#4	768	783	15
CH#5	840	858	18

Table 5: Theoretical propagation time, estimated propagation time, and their errors (T1 and T2).

accelerometer	T1		
	calculated	measured	error
CH#4	697	696	1
CH#5	768	768	0
accelerometer	T2		
	calculated	measured	error
CH#4	768	770	2
CH#5	840	837	3

CONCLUSION

As described in this paper, we explained the use of GA to reduce the computation time for detecting cracks in concrete structures. Because the use of GA reduces the computation time to 1/100 of the conventional duration, the proposed method is practical. Some experiments using a caisson show that propagation delays for the reflected wave from the joint were estimated precisely.

REFERENCES

[1] K. Preiss, "Checking of cast in place concrete piles by nuclear radiation methods," *British J. Non-Destructive Testing*, 70–76, (1971).

[2] J. K. C. Shih, R. Delpak, C. W. Hu, D. B. Tann and D. B. Moore, "The use of IR thermography in structural health monitoring," *Structural Health Monitoring and Intelligent Infrastructure*, **2**, 687–692 (2003).

[3] M. Sansalone and N. J. Carino, "Detecting delaminations in concrete slabs with and without overlays using the impact echo methods," *ACI Materials J.*, **86-M18**, 175–184 (1989).

[4] K. Kaito, M. Abe, Y. Fujino and K. Kumasaka, "Detection of internal voids in concrete structures using local vibration information," *J. Materials, Concrete Structures and Pavements*, **690/V-53**, 121–132, (2001) (in Japanese).

[5] M. Abe, S. Hongo, Y. Nemoto and Y. Chubachi, "Non-destructive technique to estimate the position of a crack in a concrete block buried in the ground," *Proc. Third International Congress on Air- and Structure-Borne Sound and Vibration*, **3**, 2045–2052, (1994).

[6] M. Abe, T. Fujioka and Y. Nagata, "Location of a defect in a concrete block by a non-destructive technique," *Acoust. Sci. & Tech.*, **23**, 308–312, (2002).

[7] M. Abe, Y. Nagata and K. Kido, "A new method to locate vibration sources by searching the minimum value of error function," *Proc. IEEE International Conf. on Acoustics, Speech, and Signal Processing*, 18B.2.1–2.4 (1986).

[8] Takeshi Murakami, Toyota Fujioka, Yoshifumi Nagata and Masato, "Nondestructive technique for estimating crack positions in a concrete structure by subtraction of the surface-wave componet," *Acoust. Sci. & Tech.*, **28**, 310–318, (2007).